

Pandiangan et al_2021

by Aprezo Pardodi Maba

Submission date: 24-Jun-2021 08:59AM (UTC+0700)

Submission ID: 1611349041

File name: Pandiangan_et_al_2021.pdf (1.18M)

Word count: 6439

Character count: 33128

PAPER · OPEN ACCESS

Physical characteristics and utilization of ZSM-5 prepared from rice husk silica and aluminum hydroxide as catalyst for transesterification of *Ricinus communis* oil

To cite this article: Kamisah Delilawati Pandiangan *et al* 2021 *Mater. Res. Express* **8** 065506

View the [article online](#) for updates and enhancements.



IOP ebooks™

Bringing together innovative digital publishing with leading authors from the global scientific community.

Start exploring the collection—download the first chapter of every title for free.



PAPER

OPEN ACCESS

RECEIVED
24 March 2021REVISED
29 April 2021ACCEPTED FOR PUBLICATION
20 May 2021PUBLISHED
23 June 2021

Original content from this work may be used under the terms of the [Creative Commons Attribution 4.0 licence](#).

Any further distribution of this work must maintain attribution to the author(s) and the title of the work, journal citation and DOI.



Physical characteristics and utilization of ZSM-5 prepared from rice husk silica and aluminum hydroxide as catalyst for transesterification of *Ricinus communis* oil

Kamisah Delilawati Pandiangan¹, Wasinton Simanjuntak¹, Sutopo Hadi¹, Ilim Ilim¹ and Henif Amrulloh²

¹ Department of Chemistry, University of Lampung, Bandar Lampung, 35144, Indonesia

² Department of Mathematics Education, Islamic Institute of Ma'arif Nahdlatul Ulama, Metro, 34118, Indonesia

E-mail: kamisah.delilawati@fmipa.unila.ac.id

Keywords: crystallization time, heterogeneous catalyst, transesterification, *Ricinus communis*

Abstract

Natural and synthetic zeolites are well-known materials sharing a wide range of applications, such as adsorbents, ion exchange, and catalysts. However, synthetic zeolites are more widely used, due to several limitations of natural zeolites, such as the presence of impurities and diverse compositions. In this study, rice husk silica (97.86% purity) and aluminum hydroxide were utilized for the preparation of ZSM-5, to study the effect of crystallization time on the physical characteristics and catalytic activity in the transesterification of *Ricinus communis* oil. The raw materials, with molar ratio of $\text{SiO}_2:0.025\text{Al}_2\text{O}_3:0.165\text{Na}_2\text{O}:25\text{H}_2\text{O}$, were subjected to crystallization at 180 °C for 48, 72, 96, and 120 h, completed by 6 h calcination at 600 °C. The formation of ZSM-5 was demonstrated by FTIR, XRD, and SEM techniques, confirmed that the formation of ZSM-5 had taken place at 48 h crystallization, with no significant change with prolonged time. The PSA indicates the existence of two clusters of particles, and the BET confirmed the existence of the zeolites as porous materials, with the sample prepared with crystallization time of 96 h had the largest surface area and smallest pore diameter. This particular sample exhibited the highest activity, resulting in 96% conversion of *Ricinus communis* oil.

1. Introduction

In general, zeolites are divided into two major groups: Natural zeolites and synthetic zeolites. These two types of zeolite share many common applications, such as adsorbents [1], ion exchange [2, 3], and catalysts [4, 5]. However, natural zeolites are known to have disadvantageous characteristics that limit their application, such as their low purity due to the presence of natural impurities, diverse compositions, and relatively low homogeneity, in terms of particle size as well as pore size. Due to such pitfalls of natural zeolites, synthetic zeolites are now more widely used, as their characteristics can be tailored to suit many specific applications, such as ion exchange [6, 7], catalysts [8, 9], membranes [10], decontamination of air using fluidized bed techniques [11], and adsorbents [12].

Chemically, zeolites are known as aluminosilicates, in appreciation of their main components being alumina and silica. Concerning these components, an array of synthetic zeolites has been prepared with different compositions, which are more commonly defined in terms of the Si/Al ratio. In addition to the composition (Si/Al) ratio, other focuses of research in the field of synthetic zeolites are raw materials (the source of silica, in particular), and the preparation technique, as they have been acknowledged as strong factors that determine the characteristics of synthetic zeolites [13].

As a silica source, both commercial silica compounds and alternative sources have been utilized to synthesize various zeolites. The most widely used commercial silica compounds are tetraethyl orthosilicate (TEOS), tetramethyl orthosilicate (TMOS), and colloidal silica (SiO_2) [14, 15]. However, due to limited availability and

the relatively high price of commercial silica, the utilization of readily available and cheaper alternative sources has also been explored in many recent studies. Some examples of non-commercial silica sources that have been studied and used are rice husk [9, 16], kaolinite [17], coal fly ash [18], and paper industry waste [19].

Besides the search for raw materials, the development of a synthesis technique is another aspect which remains a challenge for synthetic zeolites. At present, the most intensively used synthesis method is the hydrothermal [18, 20–22], although other techniques, such as direct synthesis [15], sol-gel methods [9], and microwave-assisted processes [23] have also been considered. At the industrial scale, the main method used to prepare synthetic zeolites is a hydrothermal technique using raw materials dissolved in aqueous alkaline solvent [24]. The advantages offered by this particular method are the production of high product yields, relatively low crystallization temperature, and relatively short crystallization time. For these advantageous reasons, various synthetic zeolites have been produced through the hydrothermal route; among them are zeolite-W [25], mordenite-type zeolite [26], sodalite zeolite [23], zeolite-P and zeolite-X [18], and ZSM-5 [22].

Many workers have reported the preparation of ZSM-5 involving the use of an expensive organic template as a structure-directing agent. The most widely used templates are tetrapropyl ammonium hydroxide (TPAOH) [27], tetrapropyl ammonium bromide (TPABr) [28], tetramethylammonium hydroxide (TMAOH), tetraethylammonium hydroxide (TEAOH), and tetra butyl ammonium hydroxide (TBAOH) [29]. However, the successful synthesis of ZSM-5 without the use of a template has also been reported [30, 31].

In general, the formation of zeolite is acknowledged as a process influenced by several factors, in which crystallization temperature, crystallization time, and the source of silica are the most important variables. For preparation of ZSM-5, literature information suggests that crystallization temperatures are in the range of 100 to 190 °C [32, 33]. In this study, we aimed to synthesize ZSM-5 type zeolites from RHS and $\text{Al}(\text{OH})_3$ as raw materials without the use of a template, with the composition by the general formula of $\text{SiO}_2:0.025\text{Al}_2\text{O}_3:0.165\text{Na}_2\text{O}:25\text{H}_2\text{O}$. The main objective is to evaluate the influence of the crystallization duration on the structure, the microstructure, and the catalytic activity of the products, by using them as a catalyst for transesterification reaction of *Ricinus communis* oil with methanol to produce fatty acid methyl esters (FAMEs) or biodiesel. This particular reaction was investigated considering the continuous demand for biodiesel as a renewable energy source to substitute petrochemical derived diesel. Concerning the biodiesel production technology, two aspects that remain challenging are the availability of heterogeneous catalysts and utilization of non-edible oils as a replacement of palm oil as the main feedstock currently used.

The shift from homogeneous catalyst into heterogeneous catalyst is driven by several advantages offered by heterogeneous catalyst, such as the simplicity to separate the catalyst from the product, the opportunity to reuse the catalyst, and the environmental-friendly nature of the catalyst. From raw material point of view, the use of non-edible feedstocks is useful not only to avoid the competition between energy and food but also to reduce the cost since many types of non-edible oils can be obtained with much less cost compared to edible oils. Several types of heterogeneous have been developed, and among them are zeolites, which have been used for transesterification of various non-edible feedstocks, such as *Jatropha curcas* oil using NaX, NaY, ZSM-5, beta zeolite, and mordenite [34], mustard oil using zeolite X and A [35], and sunflower oil [18]. Concerning the use of a template, we also attempted to evaluate whether ZSM-5 could be prepared from the raw materials used without involving a template.

2. Experimental

2.1. Materials

All chemicals needed to carry out the experiments were of analytical grade. Nitric acid, sodium hydroxide, aluminum hydroxide, methanol, were obtained from Merck. Rice husk was collected from a local source in Bandar Lampung, Indonesia. Oil was extracted from *Ricinus communis* beans with a hydraulic press machine, HJ-P05, manufactured by Jingdezhen Huiju Technologies Co.

2.2. Silica extraction

Silica was extracted from rice husks using the alkali extraction method with 1.5% NaOH solution, according to the sol-gel method [36]. Extraction was commenced by mixing the husk (50 grams) and 500 ml NaOH solution (1.5% by weight) in an Erlenmeyer flask. The mixture was heated to boil and kept for 30 min, then left at ambient temperature overnight. To collect the filtrate, which contained dissolved silica (silica sol), the mixture was filtered. The filtrate was neutralized using 10% HNO_3 solution, in order to convert the sol into a gel. Using hot distilled water (60 °C–70 °C), the gel was washed to remove the excess acid. The process was completed by drying the gel at 110 °C for 8 h. To determine the purity, the silica was analyzed using the XRF method with the instrument PANalytical Epsilon 3.

2.3. Synthesis of zeolite

As per the hydrothermal method reported in previous works [37, 38], a mass of 13.2 g NaOH was dissolved in 200 ml distilled water. An aliquot of 160 ml of the NaOH solution was used to dissolve 60 g of the RHS (solution A), while the rest (40 ml) was used to dissolve 3.9 g Al(OH)₃ (solution B). The raw materials solutions were thoroughly mixed by magnetic stirring for 3 h, over which 250 ml of distilled water was slowly added. The mixture was placed in a stainless steel autoclave for 24 h aging, then subjected to the crystallization process at 180 °C for 48, 72, 96, and 120 h. The products were filtered and washed, then dried at 80 °C for 6 h and, finally, subjected to 6 h calcination at 600 °C. Following the crystallization time applied, the products were specified as ZSM-5/48, ZSM-5/72, ZSM-5/96, and ZSM-5/120, respectively.

2.4. Characterization of zeolite

2.4.1. FTIR analysis

The FTIR spectrum of the sample was obtained using a Thermo Nicolet Avatar 360 type instrument. For the FTIR analysis, a sample was prepared by mixing approximately 2 mg of zeolite with 300 mg KBr in a mortar. The mixture was pressed to obtain a KBr pellet. The spectrum was generated by scanning the sample in the wavenumber range of 4000 cm⁻¹ to 400 cm⁻¹.

2.4.2. XRD analysis

The XRD diffractogram of the sample was obtained using a PANalytical Xpert MPD type instrument, operated with CuK α radiation and using diffraction angle (2θ) from 5° to 60°. The pattern of the sample was analyzed using the Match! Software (version 3.10.2.173), in order to identify the crystalline phases in the sample, and confirmed by comparing the pattern with that of the ZSM-5 standard in the International Zeolite Association (IZA) as a reference.

2.4.3. SEM analysis

Scanning electron micrographs (SEM) were captured using a ZEISS EVO MA 10 instrument, in order to recognize the morphology of the zeolites.

2.4.4. BET analysis

The Surface characteristics of the sample, including the specific surface area, total pore volume, and average pore size, were obtained according to the Brunauer, Emmett, and Teller (BET) method using a 4LX instrument. The instrument was operated using N₂ gas adsorbent at a temperature of 77.3 K, degassing temperature at 300 °C for 3 h, and an adsorption/desorption equilibrium time of 60/60 s. Data processing was carried out using the NOVA Station A instrument.

2.4.5. PSA analysis

The particle size distribution was produced with the aid of the PSA instrument Beckman Coulter LS 13 320 type.

2.5. Zeolite catalytic activity test

The activity of the synthesized ZSM-5 samples as heterogeneous catalysts were then evaluated through the transesterification of *Ricinus communis* oil (or castor oil) using methanol, to convert the oil into methyl ester; also known as biodiesel. *Ricinus communis* oil was selected, as it is a non-edible oil which naturally can grow well without strict cultivation requirements, therefore avoiding competition with the food industry and minimizing the cost of raw materials at the same time.

Each zeolite was used as a catalyst for the transesterification of *Ricinus communis* oil with methanol. The reaction was run in a 500 ml round-bottom flask with a reflux condenser. An oil/methanol volume ratio of 1:6 was used and the experiment was run at 70 °C for 7 h, with a catalyst load of 10% of the mass of the oil. After the reaction was complete, the reaction mixture was allowed to cool and then filtered into a separatory funnel. The separatory funnel was let to stand for 24 h, during which two layers formed in the funnel. The upper (biodiesel) and lower (remaining oil) layers were collected separately, and the excess methanol was removed from the upper layer by evaporation. The percentage of conversion of the oil to methyl ester was calculated using the following equation

$$\%conversion = \frac{V_i - V_f}{V_i} \times 100, \quad (1)$$

where V_i is the initial volume of oil (ml) and V_f is the volume of unreacted oil (ml). The percentage of conversion was used to compare the catalytic activities of the zeolites.

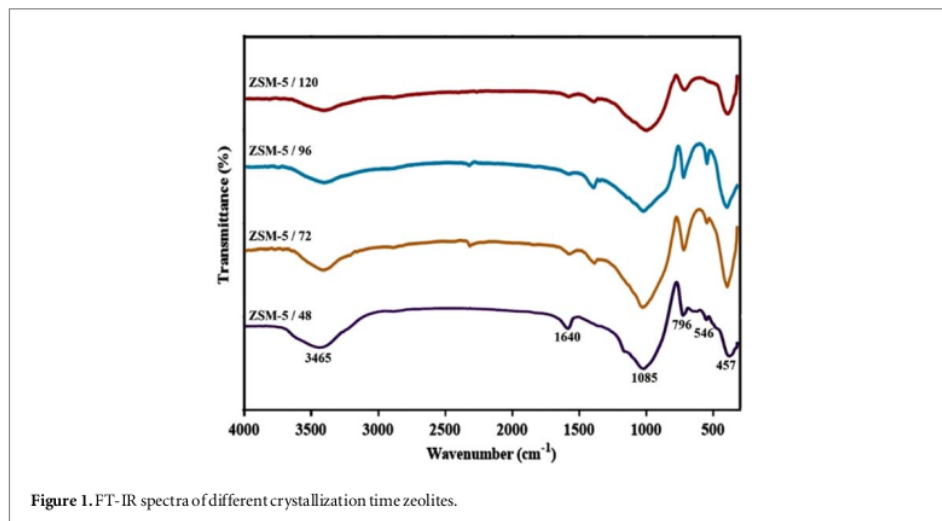


Figure 1. FT-IR spectra of different crystallization time zeolites.

Table 1. Chemical composition of the RHS.

Oxides	Relative percentage
SiO ₂	97.863
P ₂ O ₅	0.904
Al ₂ O ₃	0.540
MgO	0.313
CaO	0.246
K ₂ O	0.005
Others (relative percentage < 0.005)	0.129

2.6. Analysis of transesterification product

Analysis of transesterification product by Gas Chromatography-Mass Spectroscopy (GC-MS) was carried out using a GCMS-QP2010 SE SHIMADZU instrument. The GC column used was a 30 m long HP SMS column with internal diameter of 0.32 mm. The instrument was run at 70 eV in the EI mode, with helium as the carrier gas and nitrogen as a make up gas, with a total flow rate of 60 ml min⁻¹. Before analysis, the sample was filtered through Whatman 0.45 filter paper, followed by degassing to remove any gas from the samples.

Identification of FAMES in the transesterification product was conducted by comparing the mass spectrum of the sample with standard spectra in the MS Library System NIST62 and Wiley 7 databases. The relative quantity of each component was calculated by dividing its peak area by the total peak area.

3. Results and discussion

3.1. Chemical composition of rice husk silica

Chemical composition of the RHS as determined by XRF technique is shown in table 1.

As can be seen in table 1, the purity of the RHS produced is 97.863%, implying that the RHS can be accepted as pure silica. The purity of RHS silica produced in this study is comparable to the results by others who reported the purity of 93% [39], the purity of 96.7% [40], but higher purity (99%) was resulted by acid treatment followed by controlled combustion [41].

3.2. Characterization of zeolite

Characterization of samples using FTIR spectroscopy produced the spectra shown in figure 1. The FTIR spectra of the samples shown in figure 1 are characterized by the existence of several absorption bands, acknowledged as the characteristic vibrations of zeolite functional groups. The band located at 796 cm⁻¹ is due to the symmetric stretching mode of inter tetrahedral linkages, while that at 457 cm⁻¹ corresponds to the bending modes of O-T and O-Si-O, where T represents Al or Si. Internal asymmetric stretching of Si-O-T is characterized by the band at 1089 cm⁻¹. The absorption band at 546 cm⁻¹ is associated with pentacyl ring framework vibration, which is

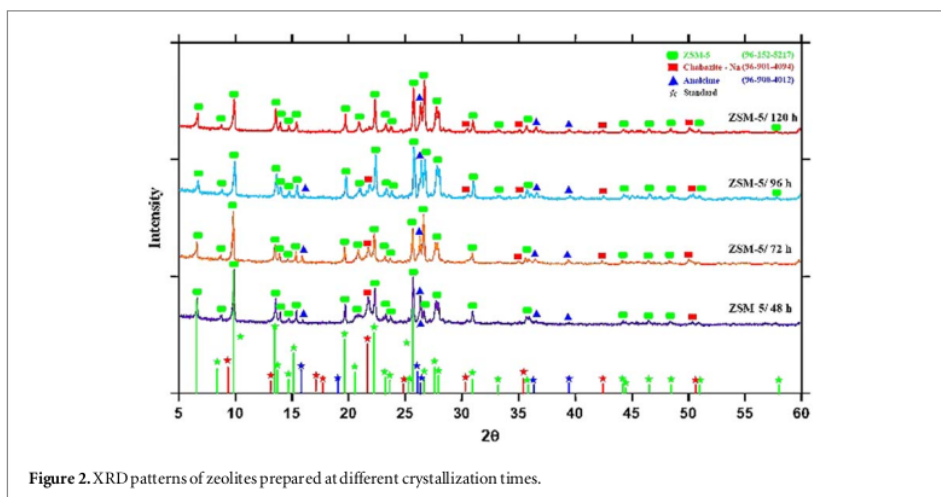


Figure 2. XRD patterns of zeolites prepared at different crystallization times.

Table 2. Comparison of the peaks of the samples with IZA data of ZSM-5 in the absence of an organic template.

IZA 2θ (°)	Sample 2θ (°)			
	ZSM-5/48	ZSM-5/72	ZSM-5/96	ZSM-5/120
9.72	9.73	9.73	9.73	9.75
6.51	6.51	6.52	6.57	6.53
13.49	13.49	13.48	13.51	13.49
25.71	25.66	25.66	25.76	25.73
8.66	8.62	8.62	8.63	8.67
22.32	22.29	22.25	22.34	22.30

characteristic of the ZSM-5 zeolite [20, 42]. The absorption band at 3456 cm^{-1} is associated with stretching vibration of the —O—H group of the water molecules adsorbed by the zeolite frame-work. The adsorbed water is supported by the absorption band located at 1640 cm^{-1} , which is assigned to the bending vibration of the molecule [30]. The existence of absorption bands representing functional groups associated with Si, O, Al, and the pentacyl ring frame-work in the spectra suggest that the reaction between silica and alumina took place during the crystallization period, in order to produce the ZSM-5 structure.

The structure of the samples investigated using XRD technique produced diffractograms are compiled in figure 2. With the aid of the Match! software (version 3.10.2.173), the phases composing the samples were identified, as included in figure 2.

The formation of ZSM-5 was also supported by XRD analysis, which indicated that ZSM-5 had been produced at 48 h and observed that the effect of crystallization time was significant in promoting the formation of the ZSM-5 structure. As can be observed, in addition to ZSM-5, chabazite and analcime phases were also identified. For this reason, the characteristics peaks for ZSM-5, chabazite, and analcime standards are included in figure 2, for comparison. For further confirmation, the diffraction data of the samples synthesized were compared with those of the ZSM-5 standard, according to the International Zeolite Association (IZA) database, as shown in table 2.

As indicated in table 2, six characteristic peaks of the ZSM-5 standard, according to the IZA database, were observed in the synthesized samples. Although a small difference in the position (2θ) was observed for some of the peaks, the difference had an acceptable value and, therefore, the data were in agreement with the results produced by the Match! Software, as previously discussed. The results obtained regarding the formation of ZSM-5 as seen by XRD are comparable to the results reported by others using other silica sources, such as kaolin [43], ludox [44], natural zeolite [45], and rice husk silica [46].

To gain more insight on the effect of crystallization times, the crystallinity of the samples was calculated adopting the method reported by others [47, 48] and the results are presented in table 3.

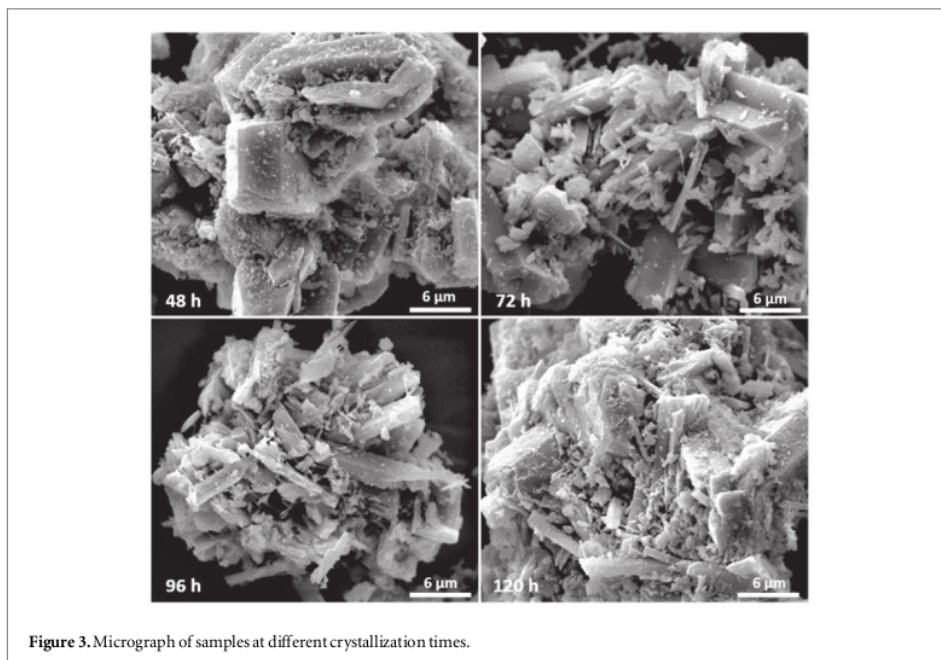


Figure 3. Micrograph of samples at different crystallization times.

Table 3. Crystallinity of the zeolites synthesized with different crystallization times.

Sample	Degree of Crystallinity
ZSM-5/48	54.42%
ZSM-5/72	69.16%
ZSM-5/96	72.56%
ZSM-5/120	89.34%

The data presented in table 3 demonstrated that the crystallinity of the sample increased with crystallization time, implying a quite significant effect of the time in the formation of crystal structure. The effect of crystallization time on the crystallinity of the samples observed in this study is in agreement with the findings reported by others [42, 49, 50]. In addition to crystallization time, crystallization temperature is another important factor in the formation of zeolite structure. For preparation of ZSM-5, literature information suggests that 180 °C is in the range of temperature commonly used [32, 33]. Another factor is the composition of the raw material, but in this study, the composition was fixed and set by the general formula of ZSM-5 ($\text{SiO}_2:0.025\text{Al}_2\text{O}_3:0.165\text{Na}_2\text{O}:25\text{H}_2\text{O}$).

Another well known characteristic of zeolites that make them valuable materials is stability. In a previous study [51], the stability of Linde Type A (LTA) zeolite was evaluated by comparing the XRD diffractogram of the sample after 4 days and that of the sample after 12 months and found that no significant difference between the diffractograms, suggesting that zeolite was stable up to 12 months after preparation. In another work, Sun *et al* [52] evaluated the stability of HZSM-5 by comparing the catalytic activity of the zeolite for liquid phase dehydration of methanol to dimethyl ether (DME) and reported that during long term test (998 to 6788 h) the zeolite retained the selectivity of more than 99.9%, which demonstrated the existence of zeolite as a highly stable material.

Figure 3 shows micrographs of the synthesized samples. As can be observed in figure 3, the samples have a heterogeneous surface, in terms of the shape and size of the particles; however, the existence of a hexagonal shape which is a characteristic shape for ZSM-5 particle [36, 53] is quite obvious.

The surface was also characterized by the presence of trapezohedral (characteristic of the analcime phase [54]) and cubic/pseudo-cubic (indicating the chabazite phase [55]) forms. The micrographs also displayed surface fractures, which was likely due to the samples being prepared without the use of an organic template, which functions to control the morphology of the crystals [56].

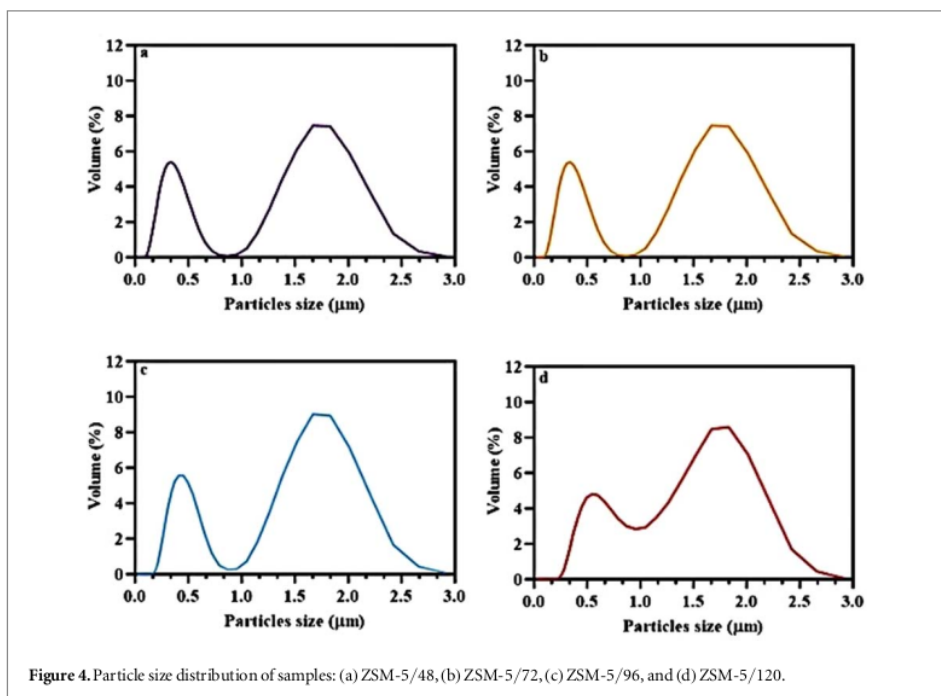


Figure 4. Particle size distribution of samples: (a) ZSM-5/48, (b) ZSM-5/72, (c) ZSM-5/96, and (d) ZSM-5/120.

Table 4. The surface area and porosity characteristics of different crystallization time zeolites.

Parameters	Sample 2 θ (°)			
	ZSM-5/48	ZSM-5/72	ZSM-5/96	ZSM-5/120
Surface area ($\text{m}^2 \text{g}^{-1}$)	7.7358	6.5689	20.2456	5.1450
Total pore volume ($\text{cm}^3 \text{g}^{-1}$)	0.0104	0.0096	0.0178	0.0052
Average pore diameter (Å)	53.932	53.932	35.164	40.302

The micrographs in figure 3, display accumulation of particles is quite significant. Particle accumulation is acknowledged to affect the catalytic activity of the zeolite, and therefore some workers have reported the method used to suppress this phenomenon. In a previous study [57] synthesis of T-type zeolite was carried out with the use of a structure-directing agent and produced the zeolite with particle sizes in the range of 120–200 nm. In another work, Wang *et al* [58] reported the particle sizes in the range of 400–500 nm of meso ZSM-5 synthesized by solid crystallization approach.

Particle size distributions of the samples, as revealed by the PSA technique, are presented in figure 4. Figure 4 displays similar profiles for the particles in all samples, characterized by the existence of two clusters of particles, indicating the existence of particle aggregates in the sample. It was also observed that, in the first three samples, the two clusters of particles were well-separated; however, in the final sample (ZSM-5/120), the two clusters overlapped, suggesting that particle agglomeration was more significant in this particular sample. The first cluster is composed of particles with diameters between 0.077 and 0.954 μm , while the second cluster has particle diameters between 0.954 and 2.920 μm .

Other physical characteristics of the samples investigated in this study, including surface area, total pore volume, and average pore diameter, were obtained using the BET method. The data are presented in table 4.

The data in table 4 illustrate that the zeolites synthesized in this study were classified as extra-large pore zeolites, as they have pore diameter $> 7.5 \text{ \AA}$ [59, 60]. The crystallization time during the hydrothermal process affects the surface area of the zeolites. The results showed that the ZSM-5/96 sample had the highest surface area (20.2456 m^2/g) and porous volume (0.0178 cm^3/g).

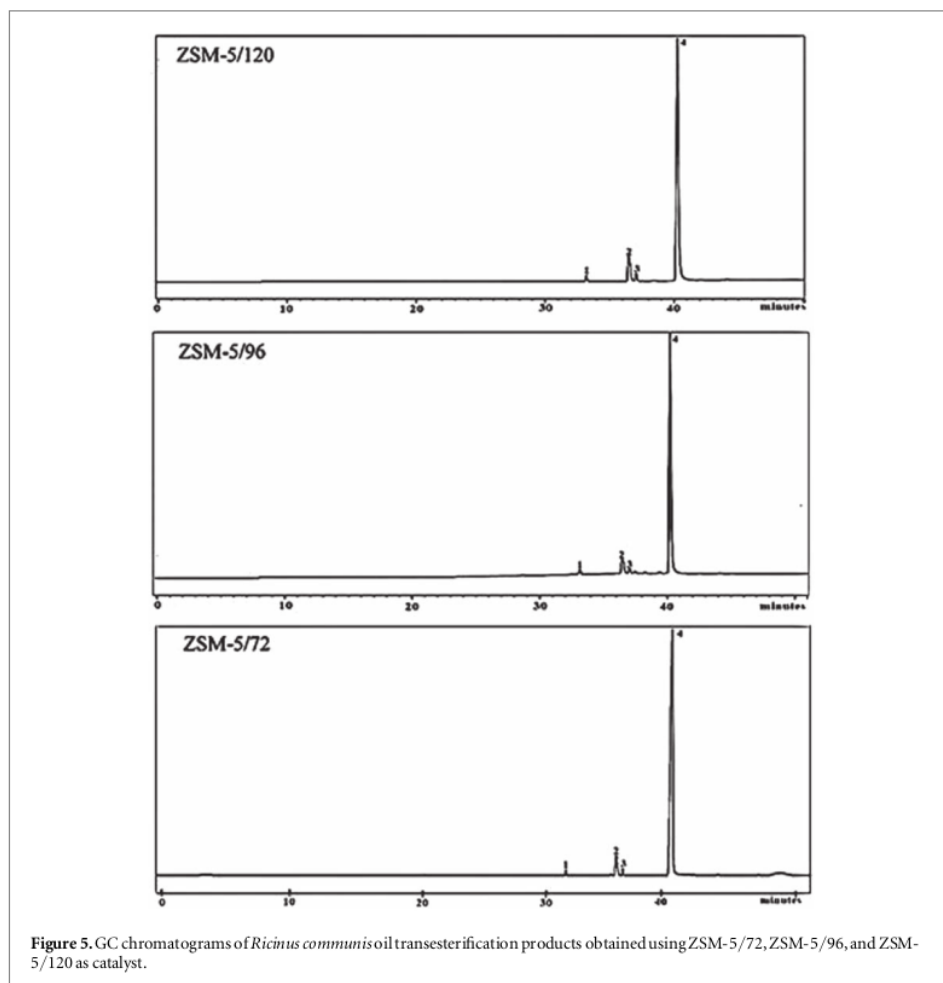


Figure 5. GC chromatograms of *Ricinus communis* oil transesterification products obtained using ZSM-5/72, ZSM-5/96, and ZSM-5/120 as catalyst.

Table 5. The components of *Ricinus communis* oil transesterification product obtained using ZSM-5/72, ZSM-5/96, and ZSM-5/120 as catalyst.

Peak number	Retention time (min)	Molecular formula	Compound name
1	33.147	C ₁₇ H ₃₄ O ₂	Methyl palmitate
2	36.515	C ₁₉ H ₃₄ O ₂	Methyl linoleaidate
3	37.059	C ₁₉ H ₃₈ O ₂	Methyl stearate
4	40.027	C ₁₉ H ₃₆ O ₃	Methylricinoleate

3.3. Zeolite catalytic activity test

Of the four ZSM-5 samples synthesized, three of them were found to exhibit appreciably high activity: ZSM-5/72, ZSM-5/96, and ZSM-5/120, with percentage of conversions of 80%, 96%, and 88%, respectively. For ZSM-5/48, the percent of conversion achieved was only 60% and, therefore, the biodiesel obtained with this particular zeolite was not analyzed further. The transesterification products obtained with three zeolites were analyzed by the GC-MS method; the chromatograms are given in figure 5.

The chromatograms in figure 5 present similar patterns, with four well-separated peaks at different retention times, indicating the existence of four chemical components in the sample. With the aid of the Library System WILEY 299 LIB and NIST 62 LIB databases, the components were identified; the results are tabulated in table 5.

As presented in table 3, the product of the transesterification reaction of *Ricinus communis* oil with methanol was a mixture of methyl esters, with methyl ricinoleate appearing as the main component. The existence of

ricinoleic acid methyl ester confirmed that the conversion of *Ricinus communis* had been achieved, as ricinoleic acid is the specific and major component of *Ricinus communis* (or castor) oil [61].

4. Conclusions

ZSM-5 zeolites were successfully synthesized from RHS and $\text{Al}(\text{OH})_3$ using a hydrothermal method in the absence of organic templates. Considering the relatively high price and toxicity of many organic templates, this study also contributes to a more cost-effective and safer method for the production of ZSM-5 zeolites with the potential to be extended to other types of synthetic zeolites. The high catalytic activity of the ZSM-5 zeolites synthesized is another important finding of the current study, considering the need for a heterogeneous catalyst to support the biodiesel industry.

Acknowledgments

Financial support from The Directorate of Higher Education, The Ministry of Research, Technology, and Higher Education, Republic of Indonesia, through the Penelitian Dasar research program, with a contract number of 857/UN26.21/PN/2019, is gratefully acknowledged. The authors appreciate the Integrated Laboratory and Center for Technology Innovation, the University of Lampung for the facility, and technical assistance to support this research project. The authors also appreciate Faulia Riyanti and Putri Damayanti for their assistance with experiments.

Data availability statement

All data that support the findings of this study are included within the article (and any supplementary files).

ORCID iDs

Kamisah Delilawati Pandiangan  <https://orcid.org/0000-0001-6347-2361>

Wasinton Simanjuntak  <https://orcid.org/0000-0001-8152-5084>

Sutopo Hadi  <https://orcid.org/0000-0001-6464-7215>

Ilim Ilim  <https://orcid.org/0000-0002-7382-6765>

Hanif Amrulloh  <https://orcid.org/0000-0001-7458-9258>

References

- [1] Moazeni M, Parastar S, Mahdavi M and Ebrahimi A 2020 Evaluation efficiency of Iranian natural zeolites and synthetic resin to removal of lead ions from aqueous solutions *Appl Water Sci* **10** 1–9
- [2] Khanmohammadi H, Bayati B, Rahbar Shahrouzi J, Babaluo A A and Ghorbani A 2019 Molecular simulation of the ion exchange behavior of Cu^{2+} , Cd^{2+} and Pb^{2+} ions on different zeolites exchanged with sodium *J. Environ. Chem. Eng.* **7** 103040
- [3] Scandelaï A P J, Zotesso J P, Jegatheesan V, Cardozo-Filho L and Tavares C R G 2020 Intensification of supercritical water oxidation (ScWO) process for landfill leachate treatment through ion exchange with zeolite *Waste Manag* **101** 259–67
- [4] Shamzhy M, Opanasenko M, Concepción P and Martínez A 2019 New trends in tailoring active sites in zeolite-based catalysts *Chem. Soc. Rev.* **48** 1095–149
- [5] Miandad R, Barakat M A, Rehan M, Aburizaiza A S, Ismail I M I and Nizami A S 2017 Plastic waste to liquid oil through catalytic pyrolysis using natural and synthetic zeolite catalysts *Waste Manag* **69** 66–78
- [6] Król M, Koleżniński A and Mozgawa W 2021 Vibrational spectra of zeolite Y as a function of ion exchange *Molecules* **26** 1–12
- [7] Savi G D, Cardoso W A, Furtado B G, Bortolotto T, Da Agostin L O V, Nones J, Zanoni E T, Montedo O R K and Angioletto E 2017 New ion-exchanged zeolite derivatives: antifungal and antimycotoxin properties against *Aspergillus flavus* and aflatoxin B1 *Mater. Res. Express* **4** 085401
- [8] Simanjuntak W, Pandiangan K D, Sembiring Z, Simanjuntak A and Hadi S 2021 The effect of crystallization time on structure, microstructure, and catalytic activity of zeolite-A synthesized from rice husk silica and food grade aluminum foil *Biomass Bioenerg* **148** 106050
- [9] Pandiangan K D, Simanjuntak W, Pratiwi E and Rilyanti M 2019 Characteristics and catalytic activity of zeolite-a synthesized from rice husk silica and aluminium metal by sol-gel method *J. Phys. Conf. Ser.* **1338** 012015
- [10] Daou J T, Santos D T, Nouali H, Josien L, Michelin L, Pieuchot L and Dutournie P 2020 Synthesis of FAU-type zeolite membranes with antimicrobial activity *Molecules* **25** 1–14
- [11] Zendehdel R, Ansari S, Sedghi R and Jafari M J 2019 Magnetic nano-zeolite Y as a novel fluidized bed for air decontamination *Int. J. Environ. Sci. Technol.* **16** 1261–8
- [12] Masala W, Vitillo J G, Mondino G, Martra G, Blom R, Grande C A and Bordiga S 2017 Conductive ZSM-5-Based Adsorbent for CO_2 Capture: Active Phase vs Monolith *Ind. Eng. Chem. Res.* **56** 8485–98
- [13] Liguori B, Aprea P, de Gennaro B, Iucolano F, Colella A and Caputo D 2019 Pozzolanic activity of zeolites: the role of Si/Al ratio *Materials* **12** 1–16

- [14] Liu Z, Shi C, Wu D, He S and Ren B 2016 A simple method of preparation of high silica zeolite Y and its performance in the catalytic cracking of cumene *J Nanotechnol* **2016** 1–6
- [15] Hosseini S, Taghizadeh M and Eliassi A 2012 Optimization of hydrothermal synthesis of H-ZSM-5 zeolite for dehydration of methanol to dimethyl ether using full factorial design *J. Nat. Gas Chem.* **21** 344–51
- [16] Klunk M A, Das M, Dasgupta S, Impiombato A N, Caetano N R, Wander P R, Roberto P W and Moraes C A M 2020 Comparative study using different external sources of aluminum on the zeolites synthesis from rice husk ash *Mater. Res. Express* **7** 015023
- [17] Pan F, Lu X, Wang Y, Chen S, Wang T and Yan Y 2014 Organic template-free synthesis of ZSM-5 zeolite from coal-series kaolinite *Mater. Lett.* **115** 5–8
- [18] Babajide O, Musyoka N, Petrik L and Ameer F 2012 Novel zeolite Na-X synthesized from fly ash as a heterogeneous catalyst in biodiesel production *Catal. Today* **190** 54–60
- [19] Moreira J C, Santa R A A B, Nones J and Riella H G 2018 Synthesis of zeolite 4a for obtaining zeolite 5A by ionic exchange for full utilization of waste from paper industry *Brazilian J Chem Eng* **35** 623–30
- [20] Corregidor P F, Acosta D E and Destéfani H A 2014 Green synthesis of ZSM-5 zeolite prepared by hydrothermal treatment of perlite Effect of chemical composition and characterization of the product *Sci Adv Mater* **6** 1203–14
- [21] Pangesti G G, Pandiangan K D, Simanjuntak W, Sasori S and Rilyanti M 2021 Synthesis of zeolite-Y from rice husk silica and food grade aluminum foil using modified hydrothermal method *J. Phys. Conf. Ser.* **1751** 012089
- [22] Rima D, Djama D and Fatma D 2019 Synthesis of high silica zeolites using a combination of pyrrolidine and tetramethylammonium as template *Mater. Res. Express* **6** 035017
- [23] Makgabatane B, Nthunya L N, Musyoka N, Dladla B S, Nxumalo E N and Mhlanga S D 2020 Microwave-assisted synthesis of coal fly ash-based zeolites for removal of ammonium from urine *RSC Adv.* **10** 2416–27
- [24] Pan T, Wu Z and Yip A C K 2019 Advances in the green synthesis of microporous and hierarchical zeolites: a short review *Catalysts* **9** 1–18
- [25] Hou J, Yuan J and Shang R 2012 Synthesis and characterization of zeolite W and its ion-exchange properties to K^+ in seawater *Powder Technol.* **226** 222–34
- [26] Gili M B Z and Conato M T 2018 Synthesis and characterization of mordenite-type zeolites with varying Si/Al ratio *Mater. Res. Express* **6** 015515
- [27] Liu Y, Luo Q, Wang G, Li X and Na P 2018 Synthesis and characterization of Y-type zeolite from coal fly ash by hydrothermal method *Mater. Res. Express* **5** 055507
- [28] Saravi Y F and Taghizadeh M 2018 Synergetic effect of Mn, Ce, Ba, and B modification and moderate desilication of nanostructured HZSM-5 catalyst on conversion of methanol to propylene *Turkish J Chem* **42** 1640–62
- [29] Ma T, Zhang L, Song Y, Shang Y, Zhai Y and Gong Y 2018 A comparative synthesis of ZSM-5 with ethanol or TPABr template: distinction of Brønsted/Lewis acidity ratio and its impact on: N-hexane cracking *Catal. Sci. Technol.* **8** 1923–35
- [30] Fouad O A, Mohamed R M, Hassan M S and Ibrahim I A 2006 Effect of template type and template/silica mole ratio on the crystallinity of synthesized nanosized ZSM-5 *Catal. Today* **116** 82–7
- [31] Zhu M H, Lu Z H, Kumakiri I, Tanaka K, Chen X S and Kita H 2012 Preparation and characterization of high water perm-selectivity ZSM-5 membrane without organic template *J Memb Sci* **415**–416 57–65
- [32] Khatamian M and Irani M 2009 Preparation and characterization of nanosized ZSM-5 zeolite using kaolin and investigation of kaolin content, crystallization time and temperature changes on the size and crystallinity of products *J. Iran. Chem. Soc.* **6** 187–94
- [33] Hartati, Permana I, Prasetyoko D and Akustia A 2016 Three-step crystallization in synthesis of ZSM-5 without organic template *AIP Conf. Proc.* **1718** 1–9
- [34] Zanetti A F, Barella R A, Pergher S B C, Treichel H, Mazutti M A, Silva E A, Oliveira J V and Oliveira D 2011 Screening, optimization and kinetics of *Jatropha curcas* oil transesterification with heterogeneous catalysts *Renew Energy* **36** 726–31
- [35] Volli V and Purkait M K 2015 Selective preparation of zeolite X and A from fly ash and its use as catalyst for biodiesel production *J. Hazard. Mater.* **297** 101–11
- [36] Pandiangan K D, Simanjuntak W, Rilyanti M, Jamarun N and Arief S 2017 Influence of kinetic variables on rubber seed oil transesterification using bifunctional catalyst CaO-MgO/SiO₂ *Orient. J. Chem.* **33** 2891–8
- [37] Kim S D, Noh S H, Seong K H and Kim W J 2004 Compositional and kinetic study on the rapid crystallization of ZSM-5 in the absence of organic template under stirring *Micropor. Mesopor. Mat.* **72** 185–92
- [38] Cheng Y, Wang L J, Li J S, Yang Y C and Sun X Y 2005 Preparation and characterization of nanosized ZSM-5 zeolites in the absence of organic template *Mater. Lett.* **59** 3427–30
- [39] Kalapathy U, Proctor A and Shultz J 2000 A simple method for production of pure silica from rice hull ash *Bioresour. Technol.* **73** 257–62
- [40] Chun J and Lee J H 2020 Recent progress on the development of engineered silica particles derived from rice husk *Sustain* **12** 1–19
- [41] Bakar R A, Yahya R and Gan S N 2016 Production of high purity amorphous silica from rice husk *Procedia Chem.* **19** 189–95
- [42] Zhao T et al 2020 Direct synthesis of hierarchical binder-free ZSM-5 and catalytic properties for MTP *Micropor Mesopor Mat* **292** 109731
- [43] Hartanto D, Kurniawati R, Pambudi A B, Utomo W P, Leaw W L and Nur H 2019 One-pot non-template synthesis of hierarchical ZSM-5 from kaolin source *Solid State Sci.* **87** 150–4
- [44] Al-Jubouri S M 2020 Synthesis of hierarchically porous ZSM-5 zeolite by self-assembly induced by aging in the absence of seeding-assistance *Micropor Mesopor Mat* **303** 1–9
- [45] Rohayati R, Krisnandi Y K and Sihombing R 2017 Synthesis of ZSM-5 zeolite using Bayat natural zeolite as silica and alumina source *AIP Conf. Proc.* **1862**, 1–5
- [46] Sari Z G L V, Younesi H and Kazemian H 2015 Synthesis of nanosized ZSM-5 zeolite using extracted silica from rice husk without adding any alumina source *Appl. Nanosci.* **5** 737–45
- [47] Van Grieken R, Sotelo J L, Menéndez J M and Melero J A 2000 Anomalous crystallization mechanism in the synthesis of nanocrystalline ZSM-5 *Micropor Mesopor Mat* **39** 135–47
- [48] Kim S, Park G, Woo M H, Kwak G and Kim S K 2019 Control of hierarchical structure and framework-Al distribution of ZSM-5 via adjusting crystallization temperature and their effects on methanol conversion *ACS Catal* **9** 2880–92
- [49] Karimi R, Bayati B, Aghdam N C, Ejtemaei M and Babaluo A A 2012 Studies of the effect of synthesis parameters on ZSM-5 nano crystalline material during template-hydrothermal synthesis in the presence of chelating agent *Powder Technol.* **229** 229–36
- [50] Mohamed R M, Fouad O A, Ismail A A and Ibrahim I A 2005 Influence of crystallization times on the synthesis of nanosized ZSM-5 *Mater. Lett.* **59** 3441–4
- [51] Belviso C, Lettino A and Cavalcante F 2018 Influence of synthesis method on LTA time-dependent stability *Molecules* **23** 1–11

- [52] Sun X, Yang Y, He Y, Zhu S and Liu Z 2020 Stability of zeolite HZSM-5 in liquid phase dehydration of methanol to dimethyl ether *Catal. Lett.* (<https://doi.org/10.1007/s10562-020-03454-y>)
- [53] Feng R, Yan X, Hu X, Zhang Y, Wu J and Yan Z 2020 Phosphorus-modified b-axis oriented hierarchical ZSM-5 zeolites for enhancing catalytic performance in a methanol to propylene reaction *Appl Catal A Gen* **594** 117464
- [54] Bortolini H R, Lima D S and Perez-Lopez O W 2020 Hydrothermal synthesis of analcime without template *J. Cryst. Growth* **532** 1–7
- [55] Dang L V, Le S T, Lobo R F and Pham T D 2020 Hydrothermal synthesis of alkali-free chabazite zeolites *J. Porous Mater.* **27** 1481–9
- [56] Mi X, Hou Z, Li X, Liu H and Guo X 2020 Synergistic effect between organic structure-directing agent and crystal seed toward controlled morphology, and bimodal pore structure of aggregated nanosized ZSM-5 *Micropor Mesopor Mat* **302** 110255
- [57] Jiang Q, Rentschler J, Sethia G, Weinman S, Perrone R and Liu K 2013 Synthesis of T-type zeolite nanoparticles for the separation of CO₂/N₂ and CO₂/CH₄ by adsorption process *Chem. Eng. J.* **230** 380–8
- [58] Wang Y, Song J, Baxter N C, Kuo G T and Wang S 2017 Synthesis of hierarchical ZSM-5 zeolites by solid-state crystallization and their catalytic properties *J. Catal.* **349** 53–65
- [59] Vinaches P, Bernardo-Gusmão K and Pergher S B C 2017 An introduction to zeolite synthesis using imidazolium-based cations as organic structure-directing agents *Molecules* **22** 1–19
- [60] Murcia B A 2013 Ordered porous nanomaterials: the merit of small *ISRN Nanotechnology* **2013** 257047
- [61] Vázquez A V, Estrada D R A, Flores A M M, Alvarado E C and Aguado C H C 2020 Transesterification of non-edible castor oil (*Ricinus communis* L.) from Mexico for biodiesel production: a physicochemical characterization *Biofuels* **11** 753–62

Pandiangan et al_2021

ORIGINALITY REPORT

10%

SIMILARITY INDEX

7%

INTERNET SOURCES

8%

PUBLICATIONS

0%

STUDENT PAPERS

PRIMARY SOURCES

1

www.jmaterenvirosci.com

Internet Source

4%

2

Winy K Maboya, Neil J Coville, Sabelo D Mhlanga. "Fabrication of chlorine nitrogen co-doped carbon nanomaterials by an injection catalytic vapor deposition method", Materials Research Express, 2021

Publication

3%

3

idoc.pub

Internet Source

3%

Exclude quotes On

Exclude matches < 3%

Exclude bibliography On